Molecular Organization and Stability of Hydrated Dispersions of Headgroup-Modified Phosphatidylethanolamine Analogues†

Rania Leventis,‡ Nola Fuller,§ R. Péter Rand,§ Philip L. Yeagle,∥ Arindam Sen,⊥ Martin J. Zuckermann,# and John R. Silvius*,‡

Departments of Biochemistry and Physics, McGill University, Montréal, Québec H3G 1Y6, Canada, Department of Biological Sciences, Brock University, St. Catharines, Ontario L2S 3A1, Canada, Department of Biochemistry, State University of New York at Buffalo, Buffalo, New York 14214, and Biophysics Department, Roswell Park Memorial Institute, Buffalo, New York 14263

Received January 15, 1991; Revised Manuscript Received April 30, 1991

ABSTRACT: Measurements of the thermotropic behavior of various headgroup-modified analogues of 1-palmitoyl-2-oleoylphosphatidylethanolamine (POPE) and of the ion-triggered destabilization of unilamellar vesicles containing these species have been correlated with X-ray diffraction measurements of the organization of hydrated dispersions of these analogues in the absence and presence of dodecane. The hexagonal II lattice repeat dimension $\bar{d}_{hex}$ for dodecane-supplemented dispersions, which reflects the optimal or "spontaneous" radius of surface curvature of the phospholipid component, is increased relative to POPE for most analogues with N-alkyl substituents or increased amino-to-phosphate group separations. Interestingly, however, POPE analogues that are alkylated on C-1 or C-2 of the ethanolamine group show *smaller* $\bar{d}_{hex}$ values (and hence smaller spontaneous radii of surface curvature) than does POPE itself, despite the greater steric bulk of their headgroups. The lamellar-to-hexagonal II transition temperatures of the various POPE analogues and their abilities to promote contact-dependent vesicle destabilization both show strong correlations with the analogues' measured $\bar{d}_{hex}$ values (and hence with their spontaneous radii of curvature). The uniformity of these correlations over a wide range of headgroup structures strongly supports, and may help to refine, recent theories which postulate that the spontaneous surface curvature of a lipid or lipid mixture is a central, *quantitative* determinant of its tendency to adopt nonlamellar phases and to undergo contact-dependent bilayer destabilization.

The demonstration that many lipid species found in biological membranes can form nonlamellar structures under physiological or near-physiological conditions (Luzzati & Husson, 1962; Cullis & de Kruijff, 1978; Gounaris et al., 1983; Albert et al., 1984) has stimulated efforts to explain the organization of various lipids in aqueous dispersions on the basis of simple, measurable structural parameters. Early models, which addressed this problem using the concept of lipid "shape" (Israelachvili et al., 1976, 1980) have been extended by recent theories that consider explicitly the relative elastic, chain-packing, "hydration" and electrostatic energies of lipids in lamellar vs nonlamellar phases (Kirk et al., 1984; Gruner et al., 1985; Anderson et al., 1988). Related analyses (Siegel, 1986a,b) have sought to predict explicitly how these properties of phospholipids govern the susceptibilities of lipid bilayers to undergo fusion and other dynamic processes in which nonlamellar structures are at least transiently formed. A key prediction of these theories is that the spontaneous curvature of a hydrated polar lipid system (i.e., the optimal radius of surface curvature that the lipids would adopt in the absence of intermonolayer packing constraints) plays a central role in determining both the system's equilibrium organization and its phase stability.

Theories such as the above, while quite general in their formulations, have to date been experimentally evaluated and refined by using data for a limited range of lipid species, primarily various phosphatidylethanolamines (PEs) and their N-methylated derivatives. Evaluation of the properties of a wider variety of phospholipids and analogues in the context of these theories offers an opportunity to test and to refine such theories further and to define better the structural features that determine the optimal packing geometry for a given phospholipid species.

In this paper, we examine how the headgroup structures of a series of analogues of 1-palmitoyl-2-oleoylphosphatidylethanolamine (POPE)[1] affect their equilibrium molecular organization in lipid/water and lipid/alkane/water dispersions as well as their thermotropic lamellar-to-nonlamellar phase transitions and their abilities to promote the contact-regulated

† This work was supported by grants from the Medical Research Council of Canada (MA-7776) and les Fonds FCAR du Québec to J.R.S. and M.J.Z., from the Natural Sciences and Engineering Research Council of Canada (OGP-0004920) to R.P.R., and from the National Institutes of Health to P.L.Y. (AI26800) and to A.S. (GM28120 and RR02685).

* Author to whom correspondence should be addressed.
‡ Department of Biochemistry, McGill University.
§ Department of Biological Sciences, Brock University.
∥ Department of Biochemistry, State University of New York at Buffalo.
⊥ Biophysics Department, Roswell Park Memorial Institute.
Department of Physics, McGill University.

[1] Abbreviations: ANTS, 8-aminonaphthalene-1,3,6-trisulfonic acid disodium salt; C_2-dimethyl-POPE, 1-palmitoyl-2-oleoylphosphatidyl(2′-amino-2′-methyl-1-propanol); C_2-ethyl-POPE, 1-palmitoyl-2-oleoylphosphatidyl(DL-2-amino-1-butanol); $\bar{d}_{hex}$ or $\bar{d}_{hex}$ (T °C), hexagonal lattice repeat spacing measured (at a temperature T °C where indicated) for fully hydrated phospholipid dispersions in the presence of 20% (w/v) dodecane; DPX, *p*-xylylenebis(pyridinium bromide); EDTA, ethylenediaminetetraacetic acid trisodium salt; PE, phosphatidylethanolamine; POPB, 1-palmitoyl-2-oleoylphosphatidyl(4-amino-1-butanol); POPC, 1-palmitoyl-2-oleoylphosphatidylcholine; POPE, 1-palmitoyl-2-oleoylphosphatidylethanolamine; POPP, 1-palmitoyl-2-oleoylphosphatidyl(3-amino-1-propanol); POPPe, 1-palmitoyl-2-oleoylphosphatidyl(5-amino-1-pentanol); Tes, *N*-[tris(hydroxymethyl)methyl]-2-aminoethanesulfonic acid sodium salt.

0006-2960/91/0430-7212$02.50/0

destabilization of unilamellar lipid vesicles. Our results indicate a strong correlation between the tendencies of different POPE analogues to form nonlamellar phases and their spontaneous curvature, as predicted by the theory of Gruner and co-workers (Kirk et al., 1984; Gruner et al., 1985). We also observe a strong relationship between the equilibrium molecular packing of different POPE analogues and their abilities to promote contact-dependent destabilization of lipid vesicles, as the theories of Siegel (1986a,b) predict on a qualitative level. The strength and regularity of these experimental correlations, across this varied family of phospholipid structures, suggest that the above theories can be extended to provide reliable *quantitative* predictions regarding the lamellar/nonlamellar interconversions of diverse phospholipids on the basis of a few fundamental (and measurable) structural parameters.

Materials and Methods

Materials. 1-Palmitoyl-2-oleoylphosphatidylcholine (POPC) was obtained from Avanti Polar Lipids (Pelham, AL). Ethanolamine and the other amino alcohols used in this study were obtained from Aldrich or Sigma; *N*-t-Boc-protected alcohols were prepared using 2-(*tert*-butoxycarbonyloxyimino)-2-phenylacetonitrile as described elsewhere (Itoh et al., 1975). Triisopropylbenzenesulfonyl chloride was purchased from Aldrich and recrystallized from hexane before use.

1-Palmitoyl-2-oleoylphosphatidylethanolamine, -(3-amino-1-propanol), -(4-amino-1-butanol), -(*N*-methylethanolamine), -(*N*-ethylethanolamine), -(*N*,*N*-diethylethanolamine), -(DL-2-amino-1-propanol), and -(DL-2-amino-1-butanol) were prepared by transphosphatidylation of 1-palmitoyl-2-oleoylphosphatidylcholine (POPC) in the presence of the appropriate amino alcohols (15–20% w/v, in 100 mM sodium acetate and 100 mM $CaCl_2$, pH 6.8) and a crude preparation of cabbage phospholipase D (Comfurius & Zwaal, 1977). 1-Palmitoyl-2-oleoylphosphatidyl(DL-1-amino-2-propanol), -(DL-2-amino-1-butanol), -(2-amino-2-methyl-1-propanol), -(*N*-propylethanolamine), -(*N*,*N*-diethylethanolamine) and -(5-amino-1-pentanol) were prepared by coupling the pyridinium salt of 1-palmitoyl-2-oleoylphosphatidic acid to the appropriate N-t-Boc-protected amino alcohol and then removing the amine-protecting group with HCl in dry chloroform, as described previously (Silvius & Gagné, 1984; Silvius et al., 1986). The crude phospholipid products were purified by silicic acid column chromatography or preparative thin-layer chromatography, as described in the above references.

Methods. Lipid samples for calorimetry were initially dispersed by vortexing in 150 mM NaCl, 10 mM Tes, and 1 mM EDTA, pH 7.4, at 0–4 °C and then incubated at this temperature for 5–7 days before thermal analysis on a Microcal MC-1 differential scanning calorimeter at a scan rate of 24 °C/h. After scanning through the temperature range of the major phase transition, samples were rapidly cooled again to 0–4 °C and rescanned within 1–2 h to 95–99 °C. Phospholipid concentrations for enthalpy determinations were standardized by organic phosphate analysis as described previously (Lowry & Tinsley, 1974; Silvius et al., 1986); lipid samples were recovered from the calorimeter cells after adding a small quantity of concentrated NaOH and mixing thoroughly to redisperse aggregated material.

^{31}P NMR spectra were obtained at 109 MHz on a JEOL FX 270 Fourier-transform NMR spectrometer, under conditions described previously (Gagné et al., 1985). Lipid samples for NMR were dispersed in 150 mM NaCl, 10 mM HEPES, and 1 mM EDTA, pH 7.4, at approximately 30 mg of lipid/mL and were incubated at 2 °C for five days before spectral analysis.

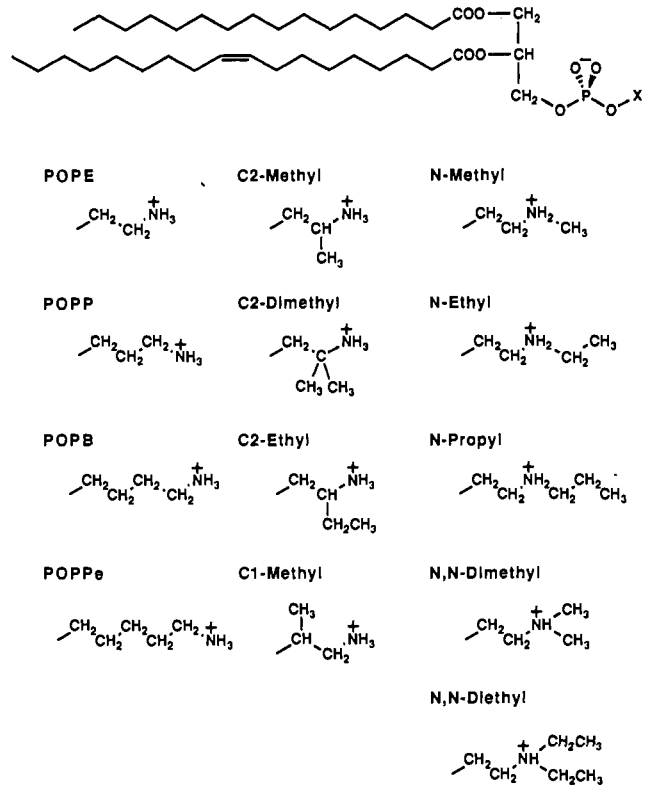

FIGURE 1: Structures of the POPE analogues examined in this study. Most POPE analogues are named in the text as derivatives of POPE, with the prefixes indicated in the figure. 1-Palmitoyl-2-oleoylphosphatidyl(3-amino-1-propanol), -(4-amino-1-butanol), and -(5-amino-1-pentanol) are designated for brevity as POPP, POPB, and POPPe, respectively.

X-ray diffraction measurements of lattice spacings of lipid dispersions were obtained as described elsewhere (Rand et al., 1990), with lipid samples containing 60 wt % water with or without 20 wt % dodecane. Lamellar phases were assigned by observing a series of three to five X-ray reflections whose relative spacings from the origin varied in the sequence 1,2,3..., while hexagonal II phases were assigned on the basis of a series of reflections whose relative spacings varied in the sequence 1, $\sqrt{3}$, 2, $\sqrt{7}$, 3, $\sqrt{11}$... X-ray determinations of the organization of *N*-propyl-POPE dispersions were carried out as described previously (Sen et al., 1990), with samples that were dispersed and preincubated for 7 days at 0–2 °C and then in some cases equilibrated further at higher temperatures as described in the text. Freeze–fracture electron microscopy was carried out as described previously (Boni & Hui, 1983).

Large unilamellar vesicles for assays of vesicle contents leakage were prepared by reverse-phase evaporation and filtration through 0.1-μm Nucleopore membranes as described previously (Wilschut et al., 1980). The vesicles were prepared in a solution containing 25 mM ANTS, 50 mM DPX, 10 mM Tes, 0.1 mM EDTA, pH 7.4, and NaCl to an osmolarity equivalent to that of 154 mM NaCl, 10 mM Tes, and 0.1 mM EDTA, pH 7.4. After gel filtration in the latter medium to remove nonencapsulated ANTS and DPX, the vesicles were diluted in this medium to 30 μM lipid for determination of the rates of calcium- and magnesium-induced contents leakage (Ellens et al., 1985; Brown & Silvius, 1989) at 33 °C.

Results

Thermotropic Behavior of POPE Analogues. The structures of the various POPE analogues examined in this study are shown in Figure 1. The thermotropic behavior of these

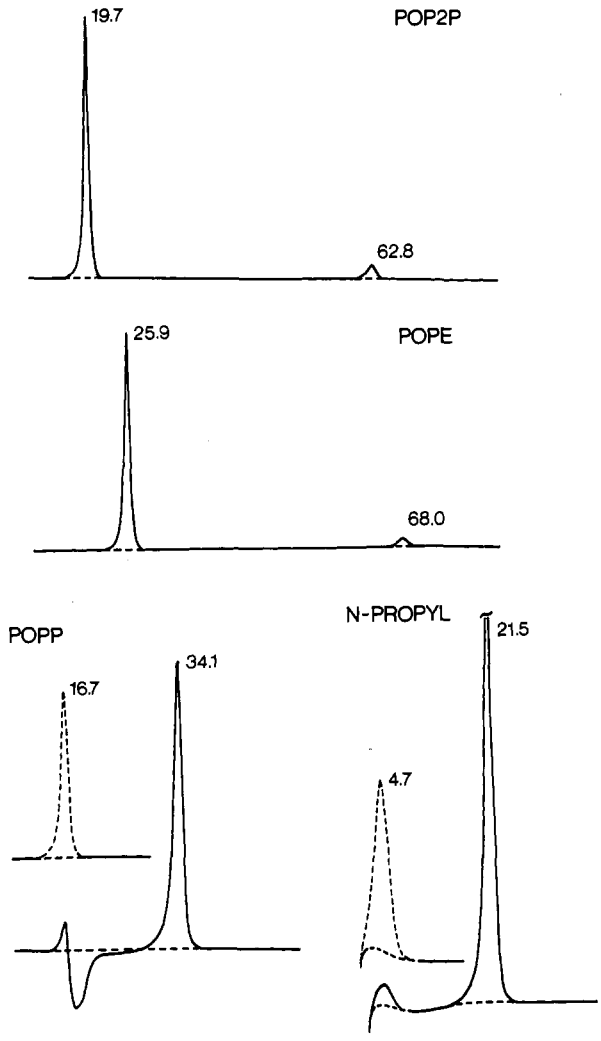

FIGURE 2: Calorimetric thermograms recorded for samples of POPE and analogues [POP2P = (*ethanolamine*)-C_2-methyl POPE; POPP = 1-palmitoyl-2-oleoylphosphatidyl(3-amino-1-propanol); N-propyl = *N*-propyl-POPE] dispersed to 5 mM lipid in 150 mM NaCl, 10 mM Tes, and 1 mM EDTA, pH 7.4. (Solid traces) Samples were dispersed at 0 °C and preincubated for 7 days at this temperature before calorimetric analysis. (Dashed traces) Repeat scans of the same samples after rapid cooling from 50 to <5 °C. Repeat scans of POPE and POP2P samples (not shown) were essentially identical with the initial scans. Experimental conditions are given under Materials and Methods.

species was examined by scanning calorimetry, using samples that were initially dispersed and incubated in buffer for 5–7 days at 0–4 °C. The preincubated samples were first scanned from 2 °C to a temperature a few degrees above the main phase transition and then rapidly cooled to 0 °C, incubated at this temperature for 1 h, and finally rescanned to 100 °C. Heating thermograms obtained by this procedure for POPE and some representative analogues are shown in Figure 2. With this protocol, POPE and several of its analogues show the same main phase transition in both heating scans, suggesting that the stable low-temperature phase for these species is the gel phase that forms rapidly on cooling from the liquid-crystalline state. For a number of other POPE analogues, however, the initial heating scan reveals a main phase transition with a markedly higher temperature and enthalpy than is observed upon subsequent cooling and rescanning (compare solid and dashed traces in Figure 2). X-ray diffraction measurements (not shown) indicated that the "high-melting" phases formed by these latter species after low-temperature preincubation were highly ordered lamellar phases similar to

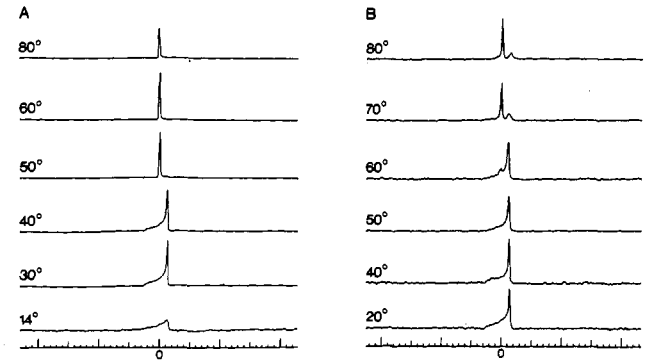

FIGURE 3: ^{31}P NMR spectra recorded at the indicated temperatures for samples of (A) *N*-propyl-POPE and (B) *N*-methyl-POPE in 150 mM NaCl, 10 mM HEPES, and 1 mM EDTA, pH 7.4, after initial dispersal and preincubation at 0–4 °C. Details of sample preparation and NMR spectral collection are given under Materials and Methods.

those previously found for analogues of other unsaturated PEs (Brown et al., 1986).

In Table I are summarized the temperatures and enthalpies measured for the melting transitions of the hydrated gel and (where observed) the more stable "high-melting" phases of various POPE analogues. As has been found for other families of PE analogues (Brown et al., 1986; Silvius et al., 1986), the transition temperature for the hydrated gel phase of these compounds (T_m[hyd]) depends chiefly, to a first approximation, on the simple steric bulk of the polar headgroup (i.e., the number of nonhydrogen atoms), while the transition temperature for the "high-melting" solid phase (T_m[crys]) is much more sensitive to fine details of the headgroup structure. This result suggests that highly specific and structure-dependent interactions between lipid headgroups may be more important in "high-melting" crystalline phases, where lipid headgroup mobility is severely restrained [this paper and Brown et al. (1986)] than in hydrated gel and liquid-crystalline lamellar phases, which permit comparatively rapid axial rotation of the lipid headgroups (Frye et al., 1985).

In addition to the major gel-to-liquid-crystalline phase transition, POPE also shows a lower enthalpy lamellar-to-hexagonal II phase transition (Cullis & de Kruijff, 1978; Epand, 1985), which occurs at 63.5 °C. Similar transitions are also observed at temperatures (T_h) below 100 °C for most of the C_1- and C_2-alkyl analogues of POPE studied (Table I). Low-enthalpy transitions were not observed above the main transition but below 100 °C for the other POPE analogues studied, even with larger-than-normal samples (20 μmol vs 5 μmol). The pattern of variation of T_h with changing lipid headgroup structure is qualitatively very similar to that observed previously for related families of analogues of dielaidoyl-PE and dioleoyl-PE (Brown et al., 1986), although the T_h values for the POPE analogues are spread over a greater temperature range.

Aqueous dispersions of *N*-monoalkyl-PEs often exhibit a particularly rich polymorphism, including the formation of nonlamellar structures whose appearance may not readily be detected by calorimetry (Gagné et al., 1985; Brown et al., 1986; Gruner et al., 1988; Siegel & Banschbach, 1990). Accordingly, we examined by ^{31}P-NMR, X-ray diffraction, and freeze–fracture electron microscopy the thermotropic behavior of the novel species *N*-propyl-POPE and, for comparison, *N*-methyl-POPE.

Samples of *N*-propyl-POPE dispersed and preincubated for 4–120 h at 0 °C showed features characteristic of a "crystalline" solid phase, including the following: a relatively weak ^{31}P NMR powder pattern, indicating strong motional

Table I: Transition Temperatures and Enthalpies for Headgroup-Modified Analogues of POPE

headgroup polar alcohol structure	T_m (hyd)[a]	ΔH (hyd)	T_m (crys)	ΔH_m (crys)	T_h
ethanolamine	25.9	7.0 ± 0.2	*b*	*b*	68.0
N-methylethanolamine	17.8	7.2 ± 0.4	*b*	*b*	
3-amino-1-propanol	16.7	6.4 ± 0.1	34.1	13.3 ± 0.2	
DL-2-amino-1-propanol	19.7	7.6 ± 0.3	*b*	*b*	62.8
DL-1-amino-2-propanol	14.0	6.9 ± 0.2	16.8	11.4 ± 0.5[c]	44.8
			30.2		
			33.0		
N,*N*-dimethylethanolamine	6.0	5.7 ± 0.2	*b*	*b*	
N-ethylethanolamine	11.8	6.5 ± 0.3	17.0	14.5 ± 0.5	
4-amino-1-butanol	8.4	5.5 ± 0.4	13.8	12.7 ± 0.7	
2-amino-2-methyl-1-propanol	13.8	8.6 ± 0.2	51.3	14.4 ± 0.3	<51.3[d]
DL-2-amino-1-butanol	8.0	6.8 ± 0.3	21.4	12.4 ± 0.6[c]	44.8
			39.6		
5-amino-1-pentanol	<2[e]	*e*	13.3	20.2 ± 2.4	
N-propylethanolamine	4.7	7.9 ± 1.0[f]	21.5	13.2 ± 0.6	
N,*N*-diethylethanolamine	<2[e]	*e*	*b*	*b*	

[a] T_m (hyd) (°C) and ΔH_m (hyd) represent the transition temperature and enthalpy for the conversion of the hydrated gel phase to the liquid-crystalline lamellar phase, and T_m (crys) and ΔH_m (crys) represent the corresponding values for conversion of the high-melting solid phase to the liquid-crystalline phase. [b] No high-melting solid phase was observed under any of the sample-preparation conditions used. [c] Total enthalpy change for the multiple transitions observed. [d] The liquid-crystalline phase formed upon melting of the hydrated gel phase rapidly relaxed to the crystalline phase, which converted directly to the hexagonal II phase at the indicated temperature. [e] No transition was observed above 2 °C, the practical lower limit of the calorimetric runs. [f] The value assigned is only approximate (with an estimated error of up to 15%) due to difficulty in baseline assignment on the lower side of the transition.

restriction of the headgroup phosphate (Figure 3A); a large number of sharp wide-angle lines (spacings 4.49, 4.31, 4.15, 3.69, 3.39 Å, ...) in the X-ray diffraction pattern (not shown); and freeze–fracture electron-microscopic images (Figure 4A) revealing mixtures of lipid aggregates with "cochleate" morphologies and multilamellar plate-like structures. Above the transition of the "high-melting" phase at 21.5 °C, *N*-propyl-POPE forms a purely lamellar liquid-crystalline phase, as indicated by ^{31}P NMR (Figure 3A), X-ray diffraction (not shown), and freeze–fracture electron microscopy (Figure 4B). At and above 50 °C, however, the ^{31}P NMR spectrum for this species collapses to a purely isotropic line shape, characteristic of rapid isotropic averaging of the headgroup phosphate orientation. Freeze–fracture images of comparable samples preincubated at 50–60 °C show very large aggregates in an amorphous state (Figure 4C), coexisting with a small proportion of small unilamellar vesicles (not shown). The amorphous state consists largely of very short bilayer segments, with irregular spacing between the lamellae; some structures similar to intermembrane attachment sites (Miller, 1980; Hui et al., 1981) are also found (Figure 4C, arrows). X-ray diffraction (not shown) gave poorly defined low-angle reflections from the latter samples, consistent with the rather disorganized structure of the lipid aggregates. Cycling of the samples up to 200 times between 0 and 80 °C did not lead to appearance of any low-angle reflections that would indicate the formation of a well-ordered "cubic" phase (not shown).

Like *N*-propyl-POPE, *N*-methyl-POPE shows a purely lamellar organization at low temperatures, with an isotropic component gradually appearing in its ^{31}P NMR spectrum as the temperature is increased (Figure 3B). However, for the N-methyl species an isotropic spectral component first appears only at 60 °C, and a major spectral component characteristic of a lamellar phase is still observed up to at least 80 °C. Freeze–fracture images of samples of *N*-methyl-POPE incubated at 50–60 °C show only multilamellar vesicles (Figure 4D).

From the above results, it is apparent that POPE derivatives with N-monoalkyl substituents larger than methyl form both high-melting "crystalline" solid phases and, at higher temperatures, localized nonlamellar structures more readily than does *N*-methyl-POPE. However, it is not clear that the former species also form well-defined nonlamellar *phases* more readily than does the N-monomethylated species.

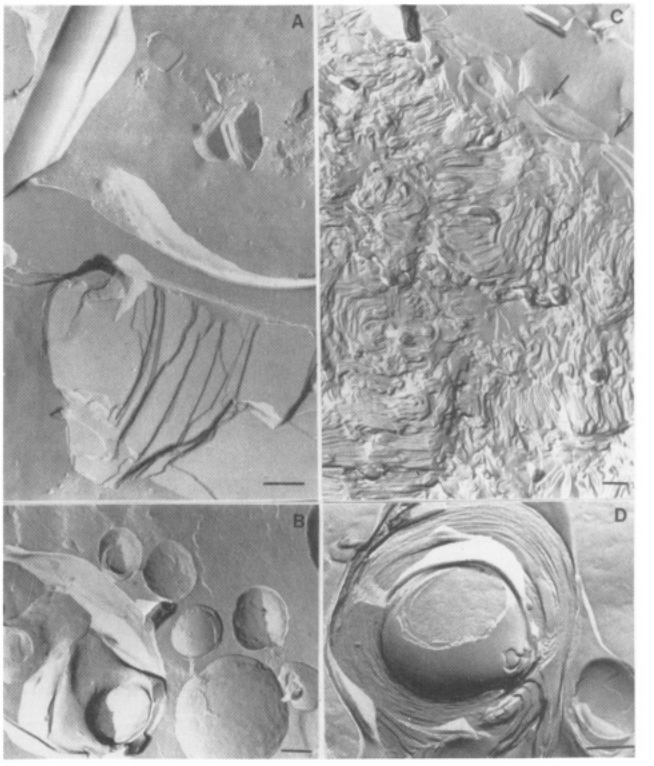

FIGURE 4: Freeze–fracture electron micrographs of dispersions of *N*-propyl-POPE and *N*-methyl-POPE at various temperatures. (A) *N*-Propyl-POPE incubated for 7 days at 0 °C. Both cochleate structures and multilamellar plate-like structures can be seen. The relative proportion of the latter structures increased with increasing time of incubation at low temperature. (B) *N*-Propyl-POPE incubated for 2 h at 30 °C. (C) *N*-Propyl-POPE incubated at 60 °C for 20 min and then quickly cooled to 50 °C just before rapid freezing. (D) *N*-Methyl-POPE incubated for 20 min at 50 °C. Scale bars are 200 nm.

X-Ray Diffraction. To examine the equilibrium dimensions of the liquid-crystalline lamellar (L_α) phases and of the "unstrained" hexagonal II cylinders formed by different POPE analogues, low-angle X-ray scattering profiles were recorded for samples of these species prepared in the presence of excess (60 wt %) water with or without 20 wt % dodecane. At 33

Table II: Lamellar Spacings (d_{lam}) and Hexagonal II Intercylinder Repeat Spacings ($\bar{d}_{hex}$) for POPE and Headgroup-Modified Analogues

headgroup	interlamellar repeat spacing[a] (nm)	hexagonal II repeat spacing (with dodecane)[a] (nm)		
	33 °C	23 °C	33 °C	50 °C
ethanolamine	5.36	8.22	7.80	
3-amino-1-propanol	5.26		8.13	7.17
4-amino-1-butanol	5.26		8.94	7.87
5-amino-1-pentanol	5.15		8.93	8.02
N-methylethanolamine	6.08	10.27	9.20	
N-ethylethanolamine	6.30	9.89	9.04	
N-propylethanolamine	6.03		7.21	6.44
N,N-dimethylethanolamine	6.53		*b*	
N,N-diethylethanolamine	6.53		*b*	
DL-2-amino-1-propanol	5.68		7.36	
DL-1-amino-2-propanol	5.23		6.93	
2-amino-2-methyl-1-propanol	4.54 (crys)[c]		*d*	6.45
DL-2-amino-1-butanol	4.92 (crys)[c]		6.59	6.03

[a] Samples were prepared as described under Materials and Methods; lamellar repeat spacings were determined for samples without dodecane, and hexagonal II intercylinder repeat spacings were determined for samples containing 20 wt % dodecane. All spacings were reproducible to within better than 0.01 nm. [b] No clear set of reflections indexing to a hexagonal lattice was found for these samples. The failure of these species to form hexagonal II cylinders probably indicates that their optimum cylinder diameters are too large to allow uniform regularly spaced hexagonal II cylinders to form even in the presence of 20 mol % alkane. [c] Samples adopted the crystalline phase at 33 °C. [d] Samples gave only reflections characteristic of a solid lamellar phase at 33 °C in the presence of dodecane.

°C, and in the absence of alkane, all of the lipid samples except (*ethanolamine*)-C_2-dimethyl- and -C_2-ethyl-POPE give low-angle reflections characteristic of the L_α phase, with the lamellar repeat distances d_{lam} (33 °C) given in Table II. All of the N-alkylated POPE derivatives examined show lamellar spacings substantially greater than that measured for POPE itself, as has been observed previously for other PEs and their N-methylated derivatives (Fuller et al., 1983; Gruner et al., 1988). By contrast, the lamellar spacings for the other types of POPE analogues examined are generally comparable to or even less than that for POPE bilayers.

Also listed in Table II are the hexagonal II repeat spacings measured for samples of POPE analogues dispersed in the presence of excess water (60 wt %) and dodecane (20 wt %). As has been shown previously (Kirk & Gruner, 1985; Siegel et al., 1989), the addition of long-chain alkanes to hydrated phospholipid dispersions can relieve packing strain at the interstices between hexagonal II cylinders and thereby allow such structures to form, adopting their optimum radius of curvature, even at temperatures where the hexagonal II phase cannot form in the absence of alkane. The repeat dimension of the hexagonal II lattice formed under these conditions, which we will designate below as $\bar{d}_{hex}$ or $\bar{d}_{hex}$ (T °C), thus reflects the spontaneous or intrinsic surface curvature of the phospholipid monolayers. For the family of POPE analogues examined here, all of which have the same hydrocarbon chains, species with smaller intrinsic radii of curvature will form cylinders of smaller diameter and hence give smaller $\bar{d}_{hex}$ values at a given temperature (Kirk & Gruner, 1985; Tate & Gruner, 1989).

POPE and most of the analogues examined readily form a hexagonal II lattice in the presence of dodecane at 33 °C. As shown in Table II, under these conditions most N-alkylated derivatives of POPE studied (with the notable exception of *N*-propyl-POPE) form hexagonal II cylinders with substantially larger dimensions than does POPE itself. Analogues of POPE with increased phospho-to-amino group separations also give greater $\bar{d}_{hex}$ (33 °C) values than does POPE. Interestingly, however, analogues of POPE bearing alkyl substituents on C-1 or C-2 of the ethanolamine moiety show significantly *smaller* $\bar{d}_{hex}$ (33 °C) values than does POPE under the same conditions. The values of $\bar{d}_{hex}$ measured for dodecane-supplemented dispersions of POPE and its analogues decrease strongly with increasing temperature (Table II). This variation is markedly (roughly 2-fold) steeper for POPE and its N-methyl derivative than for the corresponding dioleoyl species studied previously (Kirk & Gruner, 1985; Gruner et al., 1988; Tate & Gruner, 1989). Interestingly, the magnitude of the *change* in $\bar{d}_{hex}$ measured between two given temperatures (33 vs 50 °C or 23 vs 33 °C) for various POPE analogues is very regularly correlated with the value of $\bar{d}_{hex}$ measured at the lower temperature. The consistency of this relationship suggests that the profiles of $\bar{d}_{hex}$ vs temperature for different analogues represent a family of systematically related curves with a common functional form, as Tate and Gruner (1989) have suggested for dioleoyl-PE and its derivatives.

As discussed above, consideration of the thermodynamics of phospholipid interactions in lamellar and nonlamellar phases has led to the proposal that a key determinant of the proclivity of a given phospholipid to form nonlamellar structures is the spontaneous radius of surface curvature that it adopts in the absence of interstitial chain-packing stress (Kirk et al., 1984; Kirk & Gruner, 1985). This proposal is strongly supported by the data shown in Figure 5A, where the T_h values for various POPE analogues are plotted vs their measured $\bar{d}_{hex}$ (33 °C) values, which as noted above reflect their spontaneous radii of curvature. A strong correlation is evident between the two variables. While the positions of data points in Figure 5A can be assigned precisely only for POPE analogues with T_h values less than 100 °C, species giving $\bar{d}_{hex}$ (33 °C) values of 8.13 nm or greater uniformly failed to show an observable lamellar-to-hexagonal II phase transition below this temperature, as extrapolation of the data shown in Figure 5A would predict.

Destabilization of POPE Analogue-Containing Lipid Vesicles. Previously reported results (Düzgünes et al., 1981; Bentz et al., 1985; Ellens et al., 1986; Brown & Silvius, 1989) have indicated that the cation-triggered destabilization of vesicles combining anionic and neutral lipids is strongly influenced by the composition and physical properties of the neutral lipid fraction. To determine whether the physical parameters examined above could be systematically correlated with bilayer-destabilizing activity for various POPE analogues, we carried out parallel studies of the divalent-cation-mediated destabilization of large unilamellar vesicles combining these analogues with a minority fraction (25 mol %) of POPS. The sensitivity of such vesicles to divalent-cation-induced contents leakage was assayed as described previously (Silvius & Gagné, 1984; Brown & Silvius, 1989) and can be simply characterized by two parameters: first, the minimum (threshold) divalent cation concentration required to induce leakage and second, the "efficiency" of leakage, defined as the initial rate of contents release at twice the threshold concentration of the divalent cation.

As illustrated in Figure 5B, the sensitivity of POPE (analogue)/POPS vesicles to divalent-cation-induced destabilization is strongly and systematically correlated with two physical properties of the neutral lipid components that were examined in the diffraction experiments above. First, the efficiencies of divalent-cation-induced contents leakage measured for such vesicles show a strong (inverse) correlation with the value of

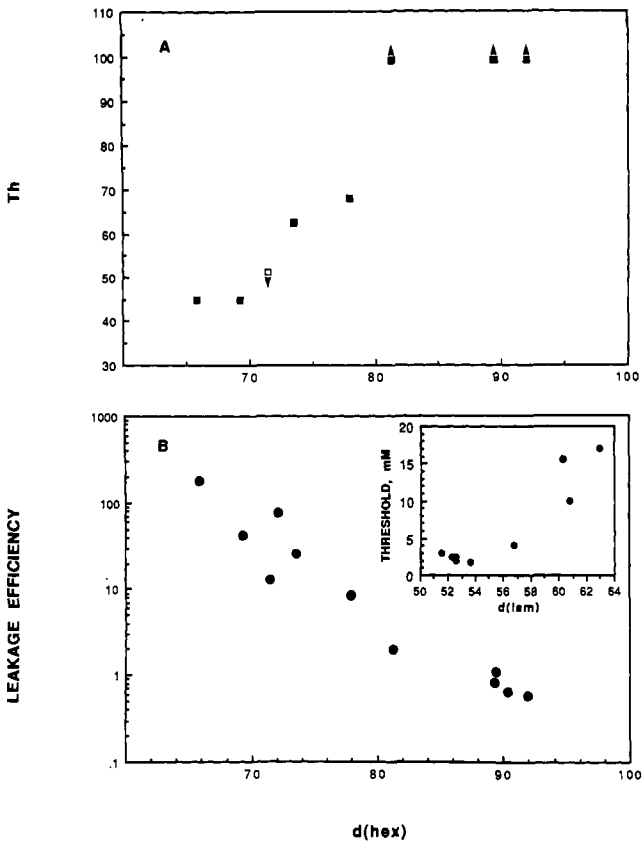

FIGURE 5: (A) Lamellar-to-hexagonal II transition temperatures T_h for dispersions of different POPE analogues plotted vs the values of $\bar{d}_{hex}$ (in Å) measured for these analogues in the presence of dodecane at 33 °C. Upward (downward) pointing arrows adjacent to symbols indicate that the lamellar-to-hexagonal II transition temperature lies above (below) the indicated temperature but cannot be assigned precisely. The open data point corresponds to C_2-dimethyl-POPE, for which the hexagonal II repeat spacing at 33 °C was estimated by extrapolation of data obtained at higher temperatures. (B) Efficiencies of calcium-induced leakage of contents from large unilamellar 75:25 POPE (analogue)/POPS vesicles at 33 °C plotted vs the values of $\bar{d}_{hex}$ (in Å) measured for the POPE analogues in the presence of dodecane at 33 °C. Details of the measurement and analysis of vesicle contents leakage rates are given in the text. Panel B (inset) shows threshold concentrations of calcium required to elicit aggregation and destabilization of 75:25 POPE (analogue)/POPS vesicles, plotted vs the lamellar spacings measured for dodecane-free aqueous dispersions of the POPE (analogue) component at 33 °C.

$\bar{d}_{hex}$ (33 °C) measured for the POPE (analogue) component. Second, as shown in the inset to Figure 5B, the threshold concentrations of divalent cations required to elicit vesicle destabilization are clearly correlated with d_{lam} (33 °C), the equilibrium lamellar-phase repeat distance measured for the POPE (analogue) component in excess water at the same reference temperature. The data shown in Figure 5B represent the results of experiments examining calcium-induced vesicle destabilization; a similar pattern of results was obtained for experiments where magnesium was used in place of calcium (not shown). Potential explanations for these correlations are discussed in the next section.

Discussion

The principle findings of this study can be summarized as follows. First, it is clear that the "dynamic shapes" of various POPE analogues, as reflected in the dimensions of the hexagonal II cylinders they form upon relaxation of interstitial packing constraints, show a complex and sometimes surprising dependence on the headgroup structure. Second, we observe a very strong correlation between the susceptibilities of different POPE analogues to form a hexagonal II phase (as reflected in their T_h values) and their values of $\bar{d}_{hex}$ (33 °C), the repeat dimension of the "unstrained" hexagonal II lattices they form at a fixed reference temperature in the presence of dodecane. Finally, we find that simple structural parameters, describing the equilibrium organization of dispersions of a given POPE analogue, are strongly correlated with kinetic parameters that reflect the tendency of the analogue to promote contact-dependent lipid vesicle destabilization. We discuss below in more detail each of these conclusions and some of their implications.

If the dimensions of the unstrained hexagonal II cylinders formed by different POPE analogues can be taken as an index of the optimal surface area requirements of their polar headgroups (Israelachvili et al., 1976, 1980), it is rather surprising that species with headgroups markedly larger than that of PE (e.g., C_2-dimethyl- or -ethyl-POPE) appear to occupy smaller surface areas in the hexagonal phase than does PE itself. This result is not inherently implausible, as the optimal surface area requirement (or the effective size) for a neutral lipid headgroup is determined by an imperfectly understood balance of several factors, including steric bulk, hydrogen-bonding ability, hydration requirements, and dipolar interactions between adjacent lipid molecules (Hauser et al., 1981; Boggs, 1987; Dill & Stigter, 1988; Seddon, 1990). Nonetheless, such results clearly challenge any simple intuitive picture of the relationship between phospholipid headgroup structure and effective size or shape that we might attempt to formulate simply from consideration of the properties of PE and its naturally occurring N-methylated derivatives. The present results support the general conclusion that structural features of a neutral lipid headgroup that decrease its strength and/or extent of hydration (e.g., favoring lipid–lipid over lipid–water polar interactions or augmenting the number or size of hydrophobic groups) tend to reduce the lipid's spontaneous radius of curvature, even when such features add appreciable steric bulk to the headgroup.

Current theories of the relative stabilities of lamellar vs inverted nonlamellar phases of uncharged amphiphiles (Kirk et al., 1984; Gruner et al., 1985; Anderson et al., 1988; Hui & Sen, 1989) stress the key importance of two factors in determining the net free energy difference between such phases. The first is the elastic energy required, in the different phases, to deform a given lipid surface from its preferred spontaneous radius of curvature. The second is the unfavorable energy of packing of acyl chains at the interstices between adjacent nonlamellar structures in inverted phases. When an analysis of these factors (Kirk et al., 1984) is applied to a series of neutral phospholipids with the same acyl chains, it is predicted that species which exhibit smaller spontaneous radii of curvature (and hence smaller $\bar{d}_{hex}$ values) under a fixed set of conditions will form an inverted-hexagonal phase more readily than will species with larger spontaneous radii of curvature. If we combine this conclusion with the suggestion of Tate and Gruner (1989) that the hexagonal lattice dimensions for related neutral phospholipids (with the same acyl chains) show closely related patterns of temperature evolution, we can make the stronger prediction that the T_h values for different POPE analogues should be strongly and monotonically correlated with their $\bar{d}_{hex}$ values measured at some reference temperature. This prediction is entirely in agreement with our experimental findings.

In order to use structural data like those examined here to predict *quantitatively* the T_h values for different POPE analogues (and hence to fit quantitatively correlations like the above), we must be able to predict the net free energy of the

hexagonal II phase (relative to the lamellar phase) as a function of the hexagonal cylinder dimensions. While most of the quantities required for this purpose are either experimentally measurable or explicitly calculable by using available theories (Kirk et al., 1984; Gruner et al. 1986; Tate & Gruner, 1989; Rand et al., 1990), one is not, namely, the energy of interstitial chain packing in the hexagonal II phase. A potentially useful simplification of this problem has recently been suggested by Lewis et al. (1989) on the basis of studies of several phosphatidylethanolamines. These authors have suggested that the free energy of the hexagonal II phase falls below that of the lamellar (L_α) phase for a given phospholipid when the optimum hexagonal II cylinder dimension for that species (which is temperature dependent) falls below a critical value that is determined by the lipid's effective acyl chain length. We are currently examining in detail the temperature variation of $\bar{d}_{hex}$ for several POPE analogues in order to test this hypothesis and to determine whether it will allow accurate prediction of the T_h values for lipids with various polar headgroups.

Our results also indicate that the ability of a given POPE analogue to promote contact-dependent destabilization of lipid vesicles is quantitatively correlated with two basic structural parameters that reflect the organization of aqueous dispersions of the analogue at equilibrium. First, the threshold concentrations of calcium or magnesium required to elicit destabilization of POPE (analogue)/POPS vesicles show a strong correlation with the equilibrium lamellar repeat distance d_{lam} measured for fully hydrated multilamellar dispersions of the neutral lipid component. This correlation cannot be rigorously accounted for on the basis of present knowledge but may be related to the basic expectation that vesicles that contain POPE analogues promoting stronger (weaker) interbilayer adhesion should require a less (more) complete neutralization of their surface charge to allow intervesicle interactions (Cevc & Marsh, 1987; Bentz & Ellens, 1988). To relate this reasonable prediction to our experimental observations, it is necessary to introduce two further assumptions: first, that the affinity of divalent cation binding is similar for the different types of POPE (analogue)/POPS vesicles, and, second, that the strength of adhesion between bilayers of different POPE analogues is (inversely) correlated with their measured d_{lam} values. The first assumption appears reasonable in view of previous results (McLaughlin et al., 1981). The second assumption, while unproven, may be expected from various theoretical considerations [see discussion in Rand et al. (1988)] and is consistent with experimental measurements for a variety of lipid systems (Lis et al., 1982; Evans & Needham, 1987; Rand & Parsegian, 1989) which show that modifications of the interfacial polar groups that reduce the interbilayer separation are accompanied by an increased adhesion energy.

We have also found in this study that the efficiencies of divalent-cation-induced contents leakage from POPE (analogue)/POPS vesicles show a strong correlation with the values of $\bar{d}_{hex}$ (33 °C) measured for the different analogues, which in turn reflect the spontaneous radii of curvature for these lipid species. The existence of such a correlation could be rationalized qualitatively by attributing vesicle leakage to fluctuations in the organization of apposed vesicle surfaces, which will vary in amplitude as a function of the proximity of the vesicle lipids to their lamellar-to-hexagonal II phase transition (Bentz et al., 1985; Ellens et al., 1986). More insight may be gained, however, from efforts to model quantitatively the mechanism of the process of contact-dependent bilayer destabilization. The theory of Siegel (1984, 1986a,b) postulates that a key step in this process is the generation and coalescence of inverted micellar intermediate (IMI) structures between apposed vesicles. While the geometry of IMI structures is of course different from that of hexagonal II cylinders, the free energy (and hence the rate) of creation of IMI's between apposed vesicle surfaces is also predicted to depend strongly on the spontaneous radius of curvature of the vesicle lipids (Siegel, 1986a,b) The strong correlation that we observe between the $\bar{d}_{hex}$ (33 °C) values for various POPE analogues (reflecting their spontaneous radii of curvature) and the rates of contact-dependent destabilization for vesicles containing these analogues agrees very well with this qualitative prediction. Refinement of theories like the above, to allow quantitative predictions of such experimental correlations, will provide a useful basis to test and to extend our current understanding of the mechanisms of contact-mediated membrane destabilization.

Acknowledgments

We thank Drs. Ruthven N. A. H. Lewis and David P. Siegel for useful discussions during the preparation of this paper.

References

Albert, A. D., Sen, A., & Yeagle, P. L. (1984) *Biochim. Biophys. Acta 771*, 28–34.

Anderson, D. M., Gruner, S. M., & Leibler, S. (1988) *Proc. Natl. Acad. Sci. U.S.A. 85*, 5364–5368.

Bentz, J., & Ellens, H. (1988) *Colloids Surf. 30*, 65–112.

Bentz, J., Ellens, H., Lai, M.-Z., & Szoka, F. C. (1985) *Proc. Natl. Acad. Sci. U.S.A. 82*, 5742–5745.

Boggs, J. M. (1987) *Biochim. Biophys. Acta 906*, 353–404.

Boni, L. T., & Hui, S. W. (1983) *Biochim. Biophys. Acta 731*, 177–185.

Brown, P. M., & Silvius, J. R. (1989) *Biochim. Biophys. Acta 980*, 181–190.

Brown, P. M., Steers, J., Hui, S. W., Yeagle, P. L., & Silvius, J. R. (1986) *Biochemistry 25*, 4259–4267.

Cevc, G., & Marsh, D. (1987) *Phospholipid Bilayers*, Wiley-Interscience, New York.

Chang, H., & Epand, R. M. (1983) *Biochim. Biophys. Acta 728*, 319–324.

Comfurius, P., & Zwaal, R. F. A. (1977) *Biochim. Biophys. Acta 488*, 36–42.

Cullis, P. R., & de Kruijff, B. (1979) *Biochim. Biophys. Acta 559*, 399–420.

Dill, K. A., & Stigter, D. (1988) *Biochemistry 27*, 3446–3453.

Düzgünes, N., Wilschut, J., Fraley, R., & Papahadjopoulos, D. (1981) *Biochim. Biophys. Acta 642*, 182–190.

Ellens, H., Szoka, F. C., & Bentz, J. (1985) *Biochemistry 24*, 3099–3106.

Ellens, H., Szoka, F. C., & Bentz, J. (1986) *Biochemistry 25*, 285–294.

Epand, R. M. (1985) *Chem. Phys. Lipids 36*, 387–393.

Evans, E., & Needham, D. (1987) *J. Phys. Chem. 91*, 4219–4228.

Frye, J., Albert, A. D., Selinsky, B. S., & Yeagle, P. L. (1985) *Biophys. J. 48*, 547–552.

Fuller, N., Miller, F., & Rand, R. P. (1983) *Biophys. J. 41*, 354a.

Gagné, J., Stamatatos, L., Diacovo, T., Hui, S. W., Yeagle, P. L., & Silvius, J. R. (1985) *Biochemistry 24*, 4400–4408.

Gounaris, K., Sen. A., Brain, A. P. R., Quinn, P. J., & Williams, W. P. (1983) *Biochim. Biophys. Acta 728*, 129–139.

Gruner, S. M., Cullis, P. R., Hope, M. J., & Tilcock, C. P. S. (1985) *Annu. Rev. Biophys. Biophys. Chem. 14*, 211–238.

Gruner, S. M., Parsegian, V. A., & Rand, R. P. (1986) *Faraday Discuss. Chem. Soc. 81*, 29–37.
Gruner, S. M., Tate, M. W., Kirk, G. L., So, P. T. C., Turner, D. C., Keane, D. T., Tilcock, C. P. S., & Cullis, P. R. (1988) *Biochemistry 27*, 2853–2866.
Hauser, H., Pascher, I., Pearson, R. H., & Sundell, S. (1981) *Biochim. Biophys. Acta 650*, 21–51.
Hui, S.-W., & Sen, A. (1989) *Proc. Natl. Acad. Sci. U.S.A. 86*, 5825–5829.
Hui, S.-W., Stewart, T. P., Boni, L. T., & Yeagle, P. L. (1981) *Science 212*, 921–923.
Israelachvili, J. N., Mitchell, D. J., & Ninham, B. W. (1976) *J. Chem. Soc. Far. Trans. 2, 72*, 1575–1586.
Israelachvili, J. N., Marcelja, S., & Horn, R. G. (1980) *Q. Rev. Biophys. 13*, 121–200.
Itoh, N., Hagiwara, D., & Kamiya, T. (1975) *Tetrahedron Lett. 16*, 4394–4395.
Kirk, G. L., Gruner, S. M. (1985) *J. Phys. (Paris) 46*, 761–769.
Kirk, G. L., Gruner, S. M., & Stein, D. L. (1984) *Biochemistry 23*, 1093–1102.
Lewis, R. N. A. H., Mannock, D. A., McElhaney, R. N., Turner, D. C., & Gruner, S. M. (1989) *Biochemistry 28*, 541–549.
Lis, L. J., McAlister, M., Fuller, N., Rand, R. P., & Parsegian, V. A. (1982) *Biophys. J. 37*, 657–666.
Lowry, R. J., & Tinsley, I. J. (1974) *Lipids 9*, 941–942.
Luzzati, V., & Husson, F. (1962) *J. Cell Biol. 12*, 207–219.
Mannock, D. A., Lewis, R. N. A. H., & McElhaney, R. N. (1990) *Biochemistry 29*, 7790–7799.
Miller, R. G. (1980) *Nature 287*, 166–167.
Rand, R. P., & Parsegian, V. A. (1989) *Biochim. Biophys. Acta 988*, 351–376.
Rand, R. P., Fuller, N., Parsegian, V. A., & Rau, D. C. (1988) *Biochemistry 27*, 7711–7722.
Rand, R. P., Fuller, N. L., Gruner, S. M., & Parsegian, V. A. (1990) *Biochemistry 29*, 76–87.
Seddon, J. M. (1990) *Biochim. Biophys. Acta 1031*, 1–69.
Sen, A., Hui, S.-W., Mannock, D. A., Lewis, R. N. A. H., & McElhaney, R. N. (1990) *Biochemistry 29*, 7799–7804.
Siegel, D. P. (1984) *Biophys. J. 45*, 399–420.
Siegel, D. P. (1986a) *Biophys. J. 49*, 1155–1170.
Siegel, D. P. (1986b) *Biophys. J. 49*, 1171–1183.
Siegel, D. P., & Banschbach, J. L. (1990) *Biochemistry 29*, 5975–5981.
Siegel, D. P., Banschbach, J., & Yeagle, P. L. (1989) *Biochemistry 28*, 5010–5019.
Silvius, J. R., & Gagné, J. (1984) *Biochemistry 23*, 3232–3240.
Silvius, J. R., Brown, P. M., & O'Leary, T. J. (1986) *Biochemistry 25*, 4249–4258.
Tate, M. W., & Gruner, S. M. (1989) *Biochemistry 28*, 4245–4253.
Wilschut, J., Düzgünes, N., Fraley, R., & Papahadjopoulos, D. (1980) *Biochemistry 19*, 6011–6021.

Membrane Binding Induces Destabilization of Cytochrome *c* Structure†

Arturo Muga,‡,§ Henry H. Mantsch,‡ and Witold K. Surewicz*,‖
Steacie Institute for Molecular Sciences and Institute for Biological Sciences, National Research Council of Canada, Ottawa, Ontario, Canada K1A 0R6

Received February 13, 1991; Revised Manuscript Received April 19, 1991

ABSTRACT: The effect of membrane binding on the structure and stability of ferricytochrome *c* was studied by Fourier-transform infrared spectroscopy and differential scanning calorimetry. Association of cytochrome *c* with phospholipid membranes containing phosphatidylglycerol as a model acidic phospholipid results in only slight, if any, perturbation of the protein secondary structure. However, upon membrane binding, there is a considerable increase in the accessibility of protein backbone amide groups to hydrogen–deuterium exchange, which suggests a lipid-mediated loosening and/or destabilization of the protein tertiary structure. A lipid-induced conformational perturbation of ferricytochrome *c* is also indicated by a marked decrease in the thermodynamic stability of the membrane-bound protein. Upon binding to membranes containing dimyristoylphosphatidylglycerol (DMPG) or dioleoylphosphatidylglycerol (DOPG) as a single lipid component, the denaturation temperature of ferricytochrome *c* decreases by approximately 30 °C. This is accompanied by a decrease in the calorimetric enthalpy of denaturation, particularly for the DMPG-associated protein. With ferricytochrome *c* bound to membranes containing a mixture of DMPG (or DOPG) and zwitterionic phosphatidylcholine, the extent of structural perturbation depends on the surface density of the negatively charged lipid head groups, becoming smaller with decreasing proportions of acidic phospholipid in the membrane. The observed destabilization of protein structure mediated by acidic phospholipids (and possibly formation of folding intermediates at the membrane surface) may represent a general property of a larger class of water-soluble proteins for which membrane binding is governed by electrostatic forces.

Cytochrome *c*, a 104 amino acid protein, is an essential component of the respiratory chain in mitochondria. Due to its location on the surface of the inner mitochondrial membrane, as well as its ability to associate with negatively charged membrane phospholipids, cytochrome *c* is considered a typical extrinsic membrane protein. In this context, cytochrome *c*/lipid systems have been studied extensively with the aim of understanding the role of phospholipids in the activation of peripherally bound proteins. Interest in the interaction between cytochrome *c* (as well as its heme-free precursor, apo-

† Issued as NRCC Publication No. 32300.
* To whom correspondence should be addressed.
‡ Steacie Institute for Molecular Sciences.
§ Supported by a NATO travel grant. Permanent address: Department of Biochemistry, University of the Basque Country, Bilbao, Spain.
‖ Institute for Biological Sciences.

0006-2960/91/0430-7219$02.50/0